ACS APPLIED MATERIALS & INTERFACES

Research Article

www.acsami.org

# Regulating Molecular Aggregations of Polymers via Ternary Copolymerization Strategy for Efficient Solar Cells

Qian Wang,[†] Yingying Wang,[§,∥] Wei Zheng,[*,†] Bilal Shahid,[§] Meng Qiu,[§] Di Wang,[†] Dangqiang Zhu,[*,§] and Renqiang Yang[*,§]

[†]College of Materials Science and Engineering, Harbin University of Science and Technology, Harbin 150080, China

[§]CAS Key Laboratory of Bio-Based Materials, Qingdao Institute of Bioenergy and Bioprocess Technology, Chinese Academy of Sciences, Qingdao 266101, China

[∥]College of Materials Science and Engineering, Qingdao University of Science and Technology, Qingdao 266042, China

*Supporting Information*



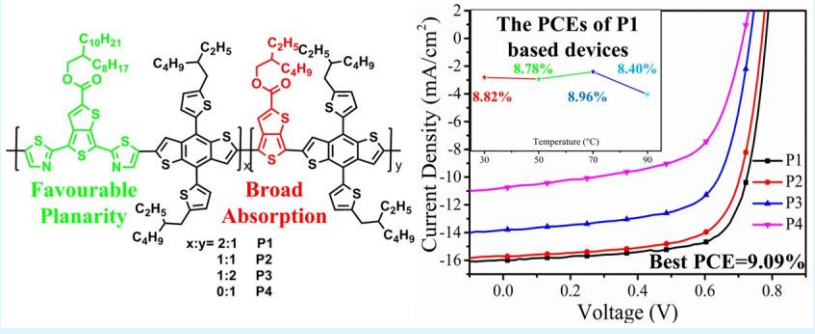


ABSTRACT: For many high-performance photovoltaic materials in polymer solar cells (PSCs), the active layers usually need to be spin-coated at high temperature due to the strong intermolecular aggregation of donor polymers, which is unfavorable in device repeatability and large-scale PSC printing. In this work, we adopted a ternary copolymerization strategy to regulate polymer solubility and molecular aggregation. A series of D−$A_1$−D−$A_2$ random polymers based on different acceptors, strong electron-withdrawing unit ester substituted thieno[3,4-*b*]thiophene (TT-E), and highly planar dithiazole linked TT-E (DTzTT) were constructed to realize the regulation of molecular aggregation and simplification of device fabrication. The results showed that as the relative proportion of TT-E segment in the backbone increased, the absorption evidently red-shifted with a gradually decreased aggregation in solution, eventually leading to the active layers that can be fabricated at low temperature. Furthermore, due to the excellent phase separation and low recombination, the optimized solar cells based on the terpolymer P1 containing 30% of TT-E segment exhibit high power conversion efficiency (PCE) of 9.09% with a significantly enhanced fill factor up to 72.86%. Encouragingly, the photovoltaic performance is insensitive to the fabrication temperature of the active layer, and it still could maintain high PCE of 8.82%, even at room temperature. This work not only develops the highly efficient photovoltaic materials for low temperature processed PSCs through ternary copolymerization strategy but also preliminarily constructs the relationship between aggregation and photovoltaic performance.

KEYWORDS: *polymer solar cells, ternary copolymerization, random terpolymer, temperature-dependent aggregation, low-temperature fabrication*

## 1. INTRODUCTION

Polymer solar cells (PSCs) are becoming a promising renewable energy technology with the particular features of solution processing to fabricate large-scale flexible modules and low energy payback time.[1−8] Over the past few years, the power conversion efficiencies (PCEs) of the single-junction fullerene PSCs has been over 11%[9] through comprehensive development of the novel donor−acceptor (D−A) copolymers design and device engineering. However, most of the high-performance photovoltaic materials usually exhibit strong intermolecular aggregation, resulting in the ITO substrate that needs to be preheated, and the blend solution of active layer must be spin-coated at high temperature (70−160 °C) during the device fabrication process, which is not appropriate for device repeatability and large-scale PSC printing.[10−23] Therefore, it is very important to develop alternative efficient donor polymers for the active layers that can be fabricated under mild processing conditions. The ternary random copolymerization could be an effective strategy to realize the excellent solubility and low aggregation degree of the responding

Received: July 3, 2017
Accepted: August 30, 2017
Published: August 30, 2017





DOI: 10.1021/acsami.7b09565
ACS Appl. Mater. Interfaces 2017, 9, 32126−32134

polymers as well as the broad absorption region and suitable molecular orbital energy levels. So far, the remarkable PCE of 10.3% has been realized among the random terpolymers (D−$A_1$−D−$A_2$ type) based on PBDT-TT system through the side chain engineering of A unit.[24] However, most work mainly focused on the regulation of the absorption and energy levels,[25−42] and very limited work referred to the regulation of intermolecular aggregation for decreasing the fabrication temperature of the devices.[43−50] Thus, it is necessary to develop further investigation of the relationship between the aggregation and structure of terpolymers for producing easily processed high-performance materials.

Previously, we reported a high-performance polymer PTBTz-2 with high PCE of 9.72% in solar cells, benefited from the deeper highest occupied molecular orbital (HOMO) energy level and larger dipole moment caused by the introduction of thiazole (see chemical structure in Scheme 1).[20] However, PTBTz-2 exhibits strong aggregation, leading to the fabrication of the active layers at high temperature (100 °C), which can be ascribed to the high planarity of thiazole (2-postion) linked thieno[3,4-*b*]thiophene (DTzTT) segment. In contrast, the copolymer PBDTTT-E-T without a π-bridge exhibits broad absorption range and good solubility but relatively low PCE of 6.21%.[51] Thus, in this work, we adopted ternary copolymerization strategy to construct a series of D−$A_1$−D−$A_2$ random polymers (P1−P3), utilizing the ester substituted TT-E and high planar DTzTT as two acceptors and benzodithiophene (2D-BDT) as donor unit, and further realized low temperature processed high-performance photovoltaic devices. The influence of relative proportions between these two acceptors on optical, electronic, and photovoltaic properties was systematically investigated. Under the comprehensive effect of two A segments, the newly synthesized terpolymers exhibit better solubility and obviously decreased aggregation in comparison with PTBTz-2, leading to the active layer fabricated at room temperature. Meanwhile, with the electron-withdrawing unit DTzTT increased, the HOMO energy levels of the terpolymers decreased, which account for the enhanced $V_{OC}$ values. More importantly, the optimized devices based on P1 containing 30% of TT-E segment show high fill factor (FF) of 72.86% and promising efficiency of 9.09%, which benefits from the low recombination, excellent phase separation, and good miscibility with $PC_{71}BM$. Moreover, it still can reach 8.82% under the fabrication of active layer at room temperature. This work provides meaningful insight into the development of highly efficient photovoltaic materials for low temperature processed PSCs by a ternary copolymerization strategy.

Scheme 1. Chemical Structures and Synthetic Route of the Terpolymers

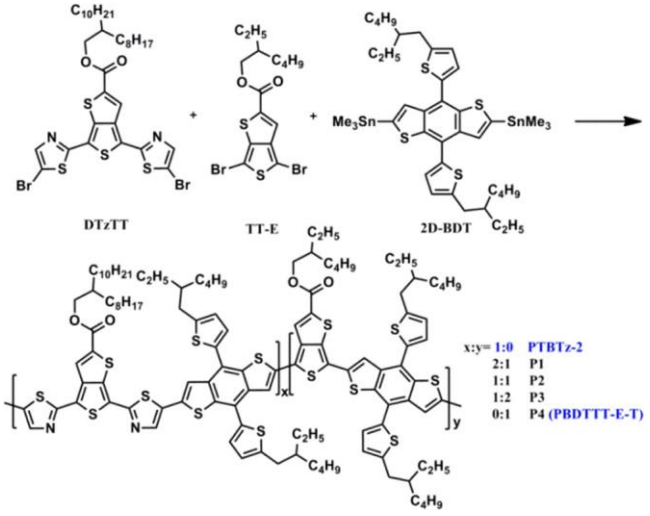


## 2. RESULT AND DISCUSSION

The synthetic methods of the monomers and copolymers can be found in previous literature.[20,51] The three terpolymers (P1−P3) were prepared through Stille coupling reaction shown in Scheme 1. In addition, the homopolymer P4 (reported as PBDTTT-E-T) was synthesized as reference. All three terpolymers exhibit good solubility in chlorobenzene (CB) under ambient conditions, while PTBTz-2 can dissolve only in hot CB and presents a gelatinous state upon cooling to room temperature (as shown in Figure S1), which makes low temperature processed device fabrication difficult. In addition, the number-average molecular weights ($M_n$) of the terpolymers can be easily tested by gel permeation chromatography (GPC) using tetrahydrofuran (THF) as eluent at 40 °C, which also confirmed the excellent solubility of the random polymers. The four polymers have similar molecular weights which guarantee their comparability (Table S1). From thermogravimetric analysis (TGA) curves shown in Figure S2, the decomposition temperatures (5% weight loss) of three terpolymers are at 325, 335, and 346 °C for P3, P2, and P1, respectively, indicating excellent thermal stabilities.

As seen in the ultraviolet−visible (UV−vis) absorption spectra of the polymers (Figure 1a), they exhibit the wide absorption region from 300 to 750 nm. The $\lambda_{onset}$ values of

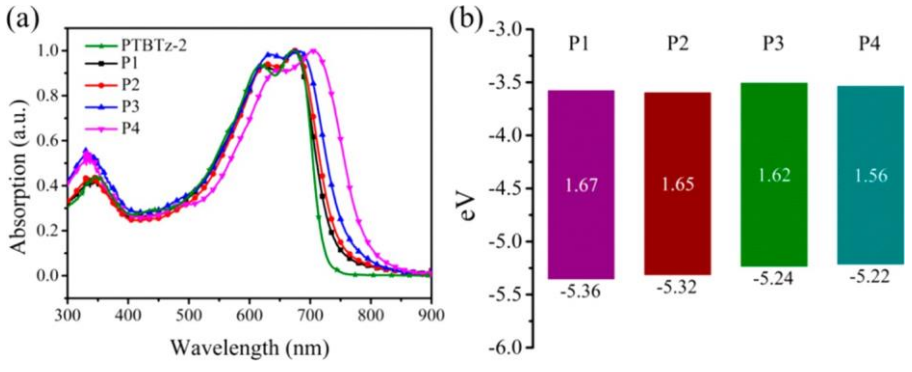


Figure 1. (a) UV−vis absorption spectra of P1−P4 and PTBTz-2 as films; (b) energy levels diagram of P1−P4.


DOI: 10.1021/acsami.7b09565
ACS Appl. Mater. Interfaces 2017, 9, 32126−32134

Table 1. Optical and Electrochemical Data for P1−P4

| | $\lambda_{max}$ (nm) | | $\lambda_{onset}$ (nm) | | | | |
|---|---|---|---|---|---|---|---|
| polymer | solution | film | solution | film | $E^{opt}$[a] (eV) | HOMO[b] (eV) | LUMO[c] (eV) |
| P1 | 623, 660 | 621, 672 | 727 | 741 | 1.67 | −5.36 | −3.69 |
| P2 | 623, 660 | 625, 675 | 728 | 747 | 1.65 | −5.32 | −3.67 |
| P3 | 623, 673 | 633, 680 | 735 | 761 | 1.62 | −5.24 | −3.62 |
| P4 | 631, 692 | 645, 704 | 772 | 794 | 1.56 | −5.22 | −3.66 |

[a]Calculated from the empirical equation $E_g^{opt} = 1240/\lambda_{onset}$. [b]Estimated from the cyclic voltammetry curve. [c]Calculated from LUMO = HOMO + $E_g^{opt}$.

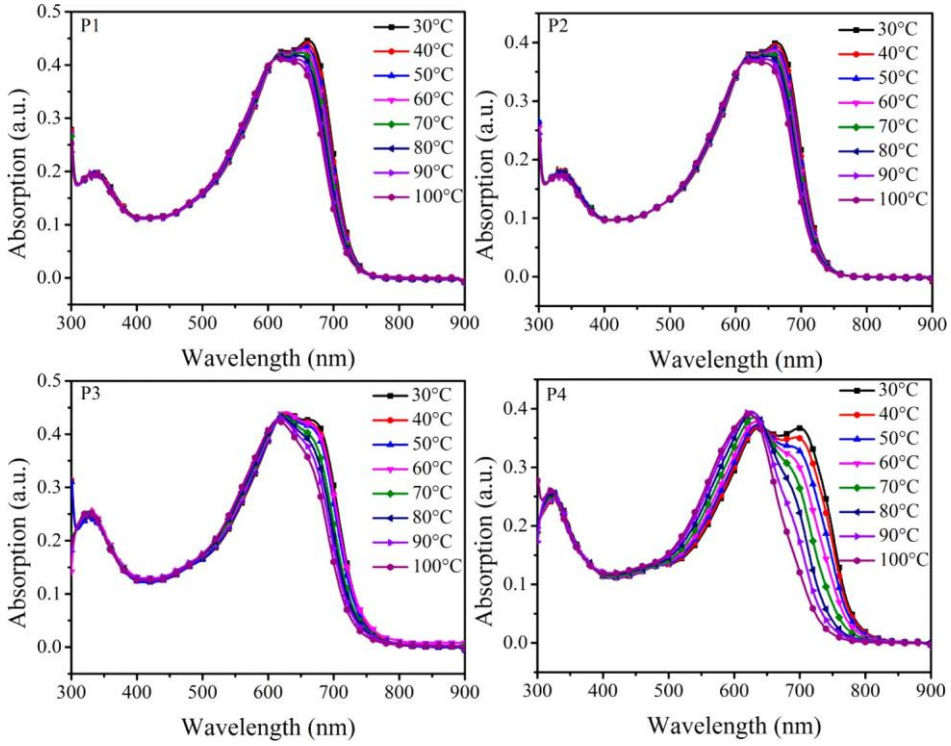


Figure 2. UV−vis absorption spectra of P1−P4 in diluted CB solution at different temperatures.

these polymers are 727, 741, 747, 761, and 794 nm, corresponding to the optical bandgaps of 1.70, 1.67, 1.65, 1.62, and 1.56 eV for PTBTz-2 and P1−P4, respectively. Clearly, the absorption region of the polymers is broadened, and the absorption maxima evidently red-shifted with the increased composition of TT-E. Meanwhile, the shoulder peaks for the four polymers imply the existence of the intermolecular interaction, which were deeply investigated in diluted solutions later. The cyclic voltammetry (CV) data of P1−P4 polymers are shown in Figure S3 and Table 1. For calibration, the ferrocene/ferrocenium ion ($Fc/Fc^+$) couple exhibits the redox potential of 0.40 V against $Ag/Ag^+$ potential and an absolute energy level of −4.80 eV to vacuum. The oxidation onset potentials are 0.96, 0.92, 0.84, and 0.82 V for P1−P4 corresponding to the HOMO level of −5.36, −5.32, −5.24, and −5.22 eV, respectively (calculated by the empirical equation: $E_{HOMO} = -e(E_{ox} + 4.4)$ V). The HOMO energy levels of the terpolymers efficiently decreased owing to the strong electron-withdrawing effect of DTzTT unit, which are beneficial to larger $V_{OC}$ values in PSCs.

To further understand the difference of aggregation degree for these 4 polymers, the temperature-dependent UV−vis absorption spectra were measured from 30 to 100 °C (Figure 2), and the detailed data are summarized in Figure S4 and Table S2. At room temperature, the terpolymers P1 and P2 exhibit 0−0 peaks ($\lambda_{0-0}$) more obvious than those of P3, indicating stronger interaction. Furthermore, it is widely considered that the intensity ratio ($R_{em}$) between $\lambda_{0-0}$ and $\lambda_{0-1}$ peak can be employed to estimate the aggregation degree of polymers.[10,52−56] Obviously, all the four polymers exhibited typical *J*-aggregates characteristic that the $R_{em}$ values almost linearly decreased as the temperature increased,[53] indicating the broken process of interchain aggregation. In detail, P1 and P2 showed strong intermolecular aggregation deduced from the high $I_{0-0}/I_{0-1}$ values of >1 at low temperature.[54] When the temperature increased to 90 °C, the $\lambda_{0-0}$ peak gradually blurred, and for P3 and P4, the shoulder peaks even disappeared at 60−70 °C. This result indicates that the existence of DTzTT segment could significantly enhance the intermolecular interaction due to its excellent planarity, and the ternary copolymerization strategy could effectively reduce the aggregation degree in comparison with that of the copolymer PTBTz-2. Furthermore, the crystalline characteristics of the neat polymers were investigated by the grazing-incidence wide-angle X-ray scattering (GIWAXS) (Figure S5). From the out-of-plane profiles, the P1 and P2 films show similar (010) peaks at $\sim q = 1.74$ Å$^{-1}$, corresponding to the π−π stacking spacing of 3.61 Å, while almost no peaks appear for P3 or P4 film, which


DOI: 10.1021/acsami.7b09565
ACS Appl. Mater. Interfaces 2017, 9, 32126−32134

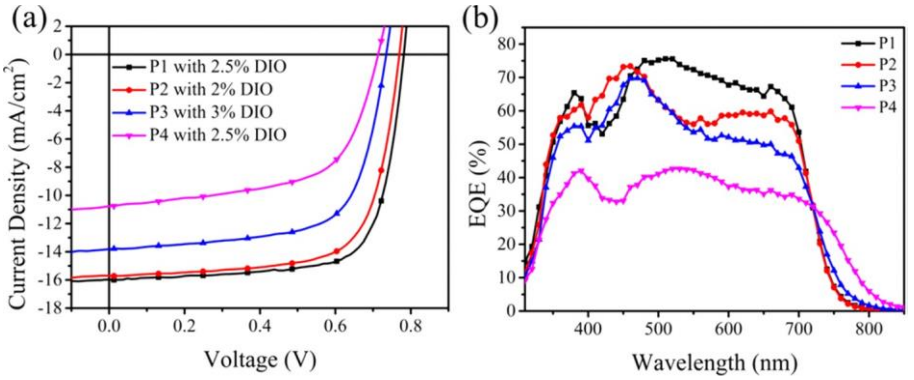


Figure 3. (a) $J-V$ curves of polymer/$PC_{71}BM$-based solar cells at optimal conditions and (b) the corresponding EQE spectra.

Table 2. Detailed Photovoltaic Parameters under Different Conditions

| polymer | DIO (%) | $V_{OC}$ (V) | $J_{SC}$ (mA/cm$^2$) | FF (%) | $PCE_{max}$ ($PCE_{ave}$)[a] (%) | thickness (nm) |
|---|---|---|---|---|---|---|
| P1 | 0 | 0.82 ± 0.02 | 7.00 ± 0.64 | 55.96 ± 2.4 | 3.23 (3.01) | 95 |
| | 2.5 | 0.78 ± 0.02 | 15.98 ± 0.65 | 72.86 ± 1.5 | 9.09 (8.78) | 98 |
| P2 | 0 | 0.81 ± 0.01 | 8.01 ± 0.56 | 52.83 ± 2.7 | 3.44 (3.29) | 101 |
| | 2 | 0.76 ± 0.02 | 15.69 ± 0.62 | 70.36 ± 1.1 | 8.49 (8.32) | 99 |
| P3 | 0 | 0.78 ± 0.02 | 7.63 ± 0.72 | 55.49 ± 2.9 | 3.32 (3.11) | 99 |
| | 3 | 0.73 ± 0.01 | 13.81 ± 0.54 | 67.27 ± 2.3 | 6.82 (6.70) | 103 |
| P4 | 0 | 0.75 ± 0.01 | 8.53 ± 0.69 | 51.32 ± 3.2 | 3.29 (3.18) | 100 |
| | 2.5 | 0.71 ± 0.01 | 10.75 ± 0.58 | 60.87 ± 2.3 | 4.67 (4.64) | 102 |
| PBDTTT-E-T[51] | 3 | 0.68 | 14.59 | 62.6 | 6.21 | |

[a]The average values in parentheses are obtained from over 15 devices.

implies relatively weaker crystallinity in the P3 or P4 films, in accordance with the result from the temperature-dependent UV−vis absorption spectra. In addition, the in-plane profiles of all films exhibit only the (100) peaks, confirming the face-on orientation in the pure film state.

To verify whether there is enough driving force to realize efficient charge transfer in fullerene-based solar cells, the photoluminescence (PL) spectra of the neat and polymer/PCBM blend films were obtained and are shown in Figure S6. The pure P1, P2, and P3 films exhibit strong PL response ranging from 720 to 800 nm with the main peaks at 750, 756, and 771 nm, respectively. When blended with $PC_{71}BM$, the PL emission peaks of the terpolymers were obviously quenched, indicating efficient charge transfer occurred. Thus, the fullerene-based PSCs with the conventional device structure of ITO/PEDOT:PSS/polymer:$PC_{71}BM$/PFN-Br/Al were fabricated. Different from that based on PTBTz-2, which must be heated at high temperature (100 °C), the active layer can be spin-coated at 50 °C from the P1−P3/$PC_{71}BM$ blend solution. The photovoltaic performances were optimized under different conditions, including various D/A ratios and additive amounts (Tables S3 and S4 and Figure S8). The current density−voltage ($J-V$) curves of PSC devices at optimal conditions are shown in Figure 3a and Figure S7, and the corresponding data are listed in Table 2. Without solvent additive, the solar cells for all polymers only exhibit poor photovoltaic performance with relatively low PCEs of <3.5%, which can be ascribed to the unfavorable phase separation discussed later. After 1,8-diiodooctane (DIO) was added, the $J_{SC}$ values and FFs were significantly enhanced for all devices, with slightly decreased $V_{OC}$ values. As a result, the best PCE for P1, P2, P3, and P4 could reach 9.09, 8.69, 6.82, and 4.67%, respectively. More specifically, as shown in Figure 4, there is a positive correlation

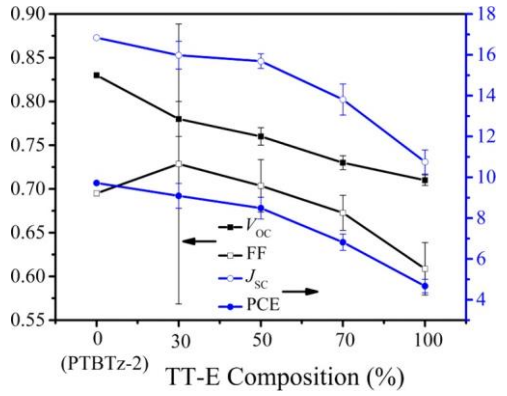


Figure 4. Dependence of $V_{OC}$, $J_{SC}$, FF, and PCE on the content of TT-E unit.

between the $V_{OC}$ values and the content of DTzTT building block, in accordance with the HOMO energy level order. Meanwhile, $J_{SC}$ values also present the same trend. Apart from the phase separation, energy transfer, and geminate recombination discussed below, here, we also proposed that it may be closely related with ground-to-excited state dipole moment ($\Delta\mu_{ge}$) of the polymer. The large calculated $\Delta\mu_{ge}$ can effectively stabilize the charge, which is in favor of fast charge separation kinetics and low recombination.[57,58] In the previous work, one main reason for PTBTz-2 with excellent photovoltaic performance was the significantly increased $\Delta\mu_{ge}$ caused by the introduction of DTzTT segment. As a result, the photovoltaic performance of three terpolymers enhanced with the increase of DTzTT segment. Encouragingly, P1 and P2 exhibited FF (72.86 and 70.36%) higher than that of the copolymer PTBTz-2 (69.5%), which may be due to the introduction of TT-E segment that adjusted the intermolecular aggregation and


DOI: 10.1021/acsami.7b09565
ACS Appl. Mater. Interfaces 2017, 9, 32126−32134

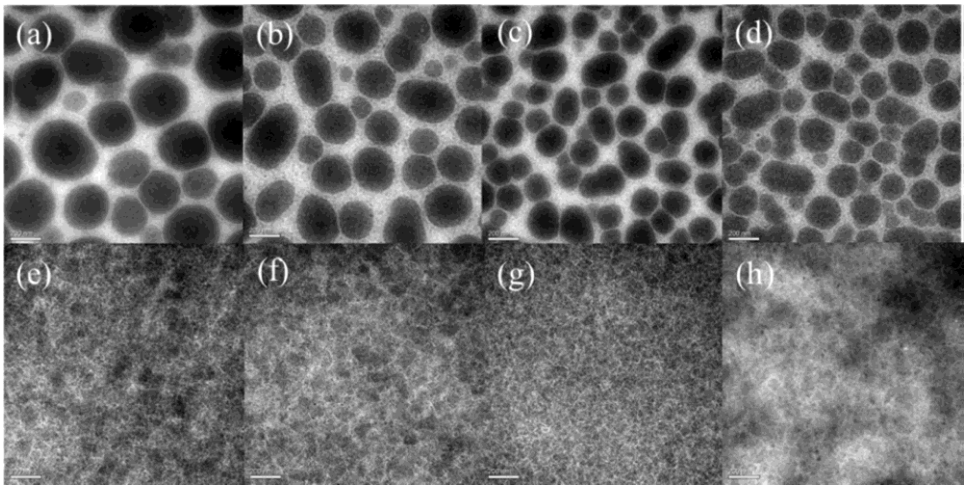


Figure 5. TEM images of P1/$PC_{71}BM$ (a and e), P2/$PC_{71}BM$ (b and f), P3/$PC_{71}BM$ (c and g), and P4/$PC_{71}BM$ (d and h) blend films without (up) and with (down) DIO.

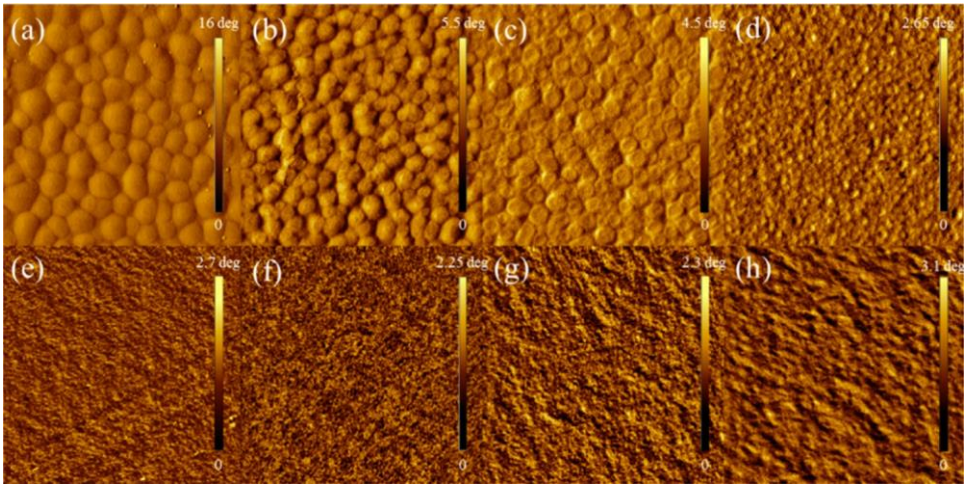


Figure 6. AFM phase images of P1/$PC_{71}BM$ (a and e), P2/$PC_{71}BM$ (b and f), P3/$PC_{71}BM$ (c and g) and P4/$PC_{71}BM$ (d and h) blend films without (up) and with (down) additive (the size is 4 × 4 μm).

enhanced the miscibility with $PC_{71}BM$.[59] More importantly, there is still a large space to improve the photovoltaic performance by the choice of various donor units, the side-chain engineering, and device structure.

External quantum efficiencies (EQEs) of the devices at the optimal conditions were measured and are shown in Figure 3b. All the devices show good photo response ranged from 300 to 750 nm, which is in accordance with the polymer/$PC_{71}BM$ blend films (Figure S9). Especially, the P1-based solar cell exhibits values from 450 to 700 nm, obviously higher than those of the others, which could account for the higher $J_{SC}$ of P1. The hole mobility of the active layers at optimal condition were investigated by space charge limited current (SCLC) method shown in Figure S10.[60] The hole mobilities for the P1−P3/$PC_{71}BM$ blend films are $1.22 \times 10^{-4}$, $1.35 \times 10^{-4}$, and $1.33 \times 10^{-4}$ $cm^2 V^{-1} S^{-1}$, respectively, which are in between those of P4 ($7.47 \times 10^{-5}$ $cm^2 V^{-1} S^{-1}$) and PTBTz-2 ($2.30 \times 10^{-4}$ $cm^2 V^{-1} S^{-1}$). Furthermore, the relationship between $V_{OC}$ and light intensity could be described as $V_{OC} \propto S\ln(I)$, and the slope $S$ is closely related with recombination.[61] As shown in Figure S11, the slopes of 1.350, 1.443, and 1.496 kT/q were calculated for P1, P2, and P3, respectively, indicating the geminate recombination was more suppressed in the P1-based devices.[62]

To further investigate the influence of the backbone structure and solvent additive, the morphology of the active layer was measured by the bright field transmission electron microscopy (TEM) and tapping-mode atom force microscopy (AFM). From the TEM and AFM phase images (Figures 5a−d and Figures 6a−d, respectively), one can obviously observe that all blend films exhibit strong aggregation with the domain sizes of >200 nm, which is not beneficial to exciton separation.[11,63] Moreover, as the TT-E segment content increased, the domain size gradually decreased, and the difference for morphology can be attributed to the aggregation properties of the four polymers originated from the composition engineering in the backbone. After the addition of DIO, the domain size significantly decreased to give more desirable morphology, accompanied with the root-mean-square (RMS) roughness of <5 nm (Figure S12), which leads to a great improvement in $J_{SC}$ values and FFs. Especially, the blend films based on P1 or P2 exhibit more favorable fibril-like structures and excellent bicontinuous interpenetrating network between the polymer and the electron acceptor, which would be the main reason for high $J_{SC}$ values in P1 and P2-based solar cells. Overall, the above results strongly confirm that the proposed ternary copolymerization strategy can adjust the intermolecular aggregation well, and the solvent


DOI: 10.1021/acsami.7b09565
ACS Appl. Mater. Interfaces 2017, 9, 32126−32134

Table 3. Photovoltaic Parameters of P1-Based PSCs at Different Processing Temperature

| temperature (°C) | $V_{OC}$ (V) | $J_{SC}$ (mA/cm$^2$) | FF (%) | $PCE_{max}$ ($PCE_{ave}$)[a] (%) | thickness (nm) |
|---|---|---|---|---|---|
| 30 | 0.77 ± 0.01 | 16.36 ± 0.17 | 69.7 ± 1.8 | 8.82 (8.80) | 100 |
| 50 | 0.77 ± 0.01 | 16.12 ± 0.38 | 69.6 ± 1.5 | 8.78 (8.74) | 103 |
| 70 | 0.77 ± 0.02 | 16.29 ± 0.36 | 70.8 ± 2.0 | 8.96 (8.90) | 97 |
| 90 | 0.78 ± 0.01 | 15.19 ± 0.26 | 70.7 ± 1.3 | 8.40 (8.28) | 98 |

[a]The average values in parentheses are obtained from over 15 devices.

additive plays a crucial role in morphology and miscibility with $PC_{71}BM$. In addition, from GIWAXS profiles of the blend films in Figure S13, in comparison with PTBTz-2-based blend film with multireflections (*h*00), it only presents weak (100) reflections in the in-plane direction, indicating distinctly weakened crystallinity. Meanwhile, the blend films based on three terpolymers P1−P3 show the similar peaks at $q = \sim 0.281$ Å$^{-1}$, corresponding to interchain distances of 22.3 Å, which are in between those of the P4-based film (21.6 Å) and PTBTz-2-based film (22.7 Å) because the lamellar distance mainly depended on the side chains length of DTzTT moiety.

On the basis of the above comprehensive analysis, we further investigated the influence of different spin-coated temperatures for the active layer on the efficiency of P1-based photovoltaic devices without ITO substrate preheated. As shown in Table 3 and Figure S14, the spin-coated temperature has little influence on the photovoltaic properties, and even when fabricated at 30 °C, the PCE still can reach at 8.82% with $V_{OC}$ of 0.77 V, $J_{SC}$ of 16.36 mA/cm$^2$, and FF of 69.7%. The above results confirmed that the ternary copolymerization strategy could effectively simplify the fabrication condition of the device via regulating the aggregation degree of the photovoltaic material.

## 3. CONCLUSION

To develop low-temperature processed high-performance photovoltaic materials, three D−$A_1$−D−$A_2$ terpolymers P1, P2, and P3 were constructed, utilizing the strong acceptor ester substituted TT-E unit and high planar DTzTT moiety as two A building blocks. The solubility, intermolecular aggregation, optical absorption, and energy levels were well-tuned with the change of TT-E segment ratios in the polymer backbones. As the TT-E segment increased, the optical absorption of the corresponding polymer obviously red-shifted with a gradually decreasing intermolecular aggregation. Consequently, the solar cells based the above terpolymers can be processed at low temperature as well as to obtain more desirable phase separation and good miscibility with fullerene acceptors in active layers. Finally, the photovoltaic device-based terpolymer P1 containing 30% of TT-E segment exhibits a high PCE of 9.09% with a $V_{OC}$ of 0.78 V, $J_{SC}$ of 15.98 mA/cm$^2$, and an enhanced FF of 72.86%, and it still can reach 8.82% under the conditions of active layer spin-coated at room temperature without annealing or substrate preheating. More importantly, the photovoltaic performance can be further improved by optimizing the side chains, donor units, and device structure. Overall, this work employed a ternary copolymerization strategy to achieve the regulation of intermolecular aggregation of the polymers and, in turn, efficient PSCs under mild processing conditions, which may be a promising characteristic in industrial application.

## 4. EXPERIMENTAL METHODS

**4.1. Synthesis of Polymers.** Bis(trimethyltin) monomer 2D-BDT (0.15 mmol) and dibromo monomer DTzTT and TT-E (in total 0.15 mmol) with different ratios were dissolved in the mixed solvent of toluene (4 mL) and DMF (1 mL). After the mixture was bubbled with argon for 15 min, the catalyst Pd $(PPh_3)_4$ (5%) was added into the mixture, which was subsequently bubbled with argon for another 40 min. After the mixture refluxed for 24 h, the crude polymer was collected from the precipitation in stirring methanol. Furthermore, Soxhlet purification was adopted by sequential extractions with methanol, hexane, and chloroform, and finally, the target polymer was obtained from the chloroform fraction by precipitation with methanol.

P1: TT-E/DTzTT ratio 1/2. black solid, yield: 80%. $^1$H NMR (600 MHz, $CDCl_3$) δ 8.21−6.25 (br), 4.64−3.94 (br), 3.43−2.60 (br), 2.45−0.31 (br).

P2: TT-E/DTzTT ratio 1/1. black solid, yield: 85%. $^1$H NMR (600 MHz, $CDCl_3$) δ 8.10−6.48 (br), 4.61−3.91 (br), 3.43−2.63 (br), 2.43−0.33 (br).

P3: TT-E/DTzTT ratio 2/1. black solid, yield: 83%. $^1$H NMR (600 MHz, $CDCl_3$) δ 8.10−6.34 (br), 4.64−3.91 (br), 3.43−2.68 (br), 2.35−0.39 (br).

P4: Black solid, yield: 87%. $^1$H NMR (600 MHz, $CDCl_3$) δ 8.10−6.48 (br), 4.69−3.91 (br), 3.43−2.60 (br), 2.29−0.45 (br).

**4.2. Photovoltaic Device Fabrication.** The PSC devices were fabricated with a configuration of ITO/PEDOT:PSS/polymer:$PC_{71}BM$/PFN-Br/Al.[64,65] The ITO glasses ($R_s$ = 15 Ω /square) were ultrasonically cleaned with cleaning agent, acetone, isopropyl alcohol, and distilled water, and after the oxygen-plasma treatment, PEDOT:PSS solution was spin-coated on ITO glasses to form the hole transport layer (about 30 nm) and then heated at 150 °C for 15 min. Further, ITO glasses need be preheated at 50 °C for 2−4 min just before spin-coating of the active layer. The polymer/$PC_{71}BM$ blend solutions (8 mg/mL for polymer, CB as the solvent) were stirred for 1 h at 70 °C. The active layers from the above blend solution were spin-coated at different speeds (optimal thickness of 90−105 nm). The effects of additive concentrations and blend ratios on device performance were also examined. In addition, for the P1-based devices at different temperatures, the blend solution was first heated under different temperatures and then spin-coated to give the active layers, just as in the aforementioned fabrication process but without ITO glass preheating. Subsequently, an ultrathin layer of PFN-Br (0.2 mg mL$^{-1}$ in methanol) was spin-coated on the active layer under 2600 rpm for 20 s. Finally, the aluminum layer (100 nm) was vacuum evaporated on the electron transport layer as cathode.

## ASSOCIATED CONTENT

### Supporting Information

The Supporting Information is available free of charge on the ACS Publications website at DOI: 10.1021/acsami.7b09565.

Experimental details, TGA curves, CV pattern, UV spectra, GIWAXS data, hole mobility, the PL spectra, AFM images, and photovoltaic data of the PSCs under different conditions (PDF)

## AUTHOR INFORMATION

### Corresponding Authors

*E-mail: zhengwei1972@sina.com.

*E-mail: zhudq@qibebt.ac.cn.

*E-mail: yangrq@qibebt.ac.cn.



DOI: 10.1021/acsami.7b09565
ACS Appl. Mater. Interfaces 2017, 9, 32126−32134

ORCID
Bilal Shahid: 0000-0003-1194-7702
Renqiang Yang: 0000-0001-6794-7416

Notes

The authors declare no competing financial interest.

## ACKNOWLEDGMENTS

The authors are deeply grateful to the National Natural Science Foundation of China (Grants 21604092 and 51573205), the China Postdoctoral Science Foundation (Grant 2017M610453), the Shandong Provincial Natural Science Foundation (Grant ZR2016BB33), and the Science and Technology Innovation Talents of Harbin (Grant 2013RFXXJ004) for financial support.

## REFERENCES

(1) Li, G.; Zhu, R.; Yang, Y. Polymer Solar Cells. *Nat. Photonics* 2012, *6*, 153−161.
(2) Søndergaard, R.; Hösel, M.; Angmo, D.; Larsen-Olsen, T. T.; Krebs, F. C. Roll-to-Roll Fabrication of Polymer Solar Cells. *Mater. Today* 2012, *15*, 36−49.
(3) Yu, G.; Gao, J.; Hummelen, J. C.; Wudl, F.; Heeger, A. J. Polymer Photovoltaic Cells-Enhanced Efficiencies via a Network of Internal Donor-Acceptor Heterojunctions. *Science* 1995, *270*, 1789−1791.
(4) Li, Y. Molecular Design of Photovoltaic Materials for Polymer Solar Cells: Toward Suitable Electronic Energy Levels and Broad Absorption. *Acc. Chem. Res.* 2012, *45*, 723−733.
(5) Chen, J.; Cao, Y. Development of Novel Conjugated Donor Polymers for High-Efficiency Bulk-Heterojunction Photovoltaic Devices. *Acc. Chem. Res.* 2009, *42*, 1709−1718.
(6) Hu, Z.; Ying, L.; Huang, F.; Cao, Y. Towards a Bright Future: Polymer Solar Cells with Power Conversion Efficiencies Over 10%. *Sci. China: Chem.* 2017, *60*, 571−582.
(7) Etxebarria, I.; Ajuria, J.; Pacios, R. Solution-Processable Polymeric Solar Cells: a Review on Materials, Strategies and Cell Architectures to Overcome 10%. *Org. Electron.* 2015, *19*, 34−60.
(8) Zhang, F.; Inganas̈, O.; Zhou, Y.; Vandewal, K. Development of Polymer−Fullerene Solar Cells. *Natl. Sci. Rev.* 2016, *3*, 222−239.
(9) Zhao, J.; Li, Y.; Yang, G.; Jiang, K.; Lin, H.; Ade, H.; Ma, W.; Yan, H. Efficient Organic Solar Cells Processed from Hydrocarbon Solvents. *Nat. Energy* 2016, *1*, 15027.
(10) Chen, Z.; Cai, P.; Chen, J.; Liu, X.; Zhang, L.; Lan, L.; Peng, J.; Ma, Y.; Cao, Y. Low Band-Gap Conjugated Polymers with Strong Interchain Aggregation and Very High Hole Mobility Towards Highly Efficient Thick-Film Polymer Solar Cells. *Adv. Mater.* 2014, *26*, 2586−2591.
(11) Liu, Y.; Zhao, J.; Li, Z.; Mu, C.; Ma, W.; Hu, H.; Jiang, K.; Lin, H.; Ade, H.; Yan, H. Aggregation and Morphology Control Enables Multiple Cases of High-Efficiency Polymer Solar Cells. *Nat. Commun.* 2014, *5*, 5293.
(12) Li, Z.; Lin, H.; Jiang, K.; Carpenter, J.; Li, Y.; Liu, Y.; Hu, H.; Zhao, J.; Ma, W.; Ade, H.; Yan, H. Dramatic Performance Enhancement for Large Bandgap Thick-Film Polymer Solar Cells Introduced by a Difluorinated Donor Unit. *Nano Energy* 2015, *15*, 607−615.
(13) Ma, T.; Jiang, K.; Chen, S.; Hu, H.; Lin, H.; Li, Z.; Zhao, J.; Liu, Y.; Chang, Y.-M.; Hsiao, C.-C.; Yan, H. Efficient Low-Bandgap Polymer Solar Cells with High Open-Circuit Voltage and Good Stability. *Adv. Energy Mater.* 2015, *5*, 1501282.
(14) Ma, W.; Yang, G.; Jiang, K.; Carpenter, J. H.; Wu, Y.; Meng, X.; McAfee, T.; Zhao, J.; Zhu, C.; Wang, C.; Ade, H.; Yan, H. Influence of Processing Parameters and Molecular Weight on the Morphology and Properties of High-Performance PffBT4T-2OD:$PC_{71}BM$ Organic Solar Cells. *Adv. Energy Mater.* 2015, *5*, 1501400.
(15) Jin, Y.; Chen, Z.; Dong, S.; Zheng, N.; Ying, L.; Jiang, X. F.; Liu, F.; Huang, F.; Cao, Y. A Novel Naphtho[1,2-*c*:5,6-*c*′]Bis([1,2,5]-Thiadiazole)-Based Narrow-Bandgap π-Conjugated Polymer with Power Conversion Efficiency Over 10%. *Adv. Mater.* 2016, *28*, 9811−9818.
(16) Kawashima, K.; Fukuhara, T.; Suda, Y.; Suzuki, Y.; Koganezawa, T.; Yoshida, H.; Ohkita, H.; Osaka, I.; Takimiya, K. Implication of Fluorine Atom on Electronic Properties, Ordering Structures, and Photovoltaic Performance in Naphthobisthiadiazole-Based Semiconducting Polymers. *J. Am. Chem. Soc.* 2016, *138*, 10265−10275.
(17) Liu, D.; Zhu, Q.; Gu, C.; Wang, J.; Qiu, M.; Chen, W.; Bao, X.; Sun, M.; Yang, R. High-Performance Photovoltaic Polymers Employing Symmetry-Breaking Building Blocks. *Adv. Mater.* 2016, *28*, 8490−8498.
(18) Liu, J.; Chen, S.; Qian, D.; Gautam, B.; Yang, G.; Zhao, J.; Bergqvist, J.; Zhang, F.; Ma, W.; Ade, H.; Inganas̈, O.; Gundogdu, K.; Gao, F.; Yan, H. Fast Charge Separation in a Non-Fullerene Organic Solar Cell with a Small Driving Force. *Nat. Energy* 2016, *1*, 16089.
(19) Zhang, Z.; Lu, Z.; Zhang, J.; Liu, Y.; Feng, S.; Wu, L.; Hou, R.; Xu, X.; Bo, Z. High Efficiency Polymer Solar Cells Based on Alkylthio Substituted Benzothiadiazole-Quaterthiophene Alternating Conjugated Polymers. *Org. Electron.* 2017, *40*, 36−41.
(20) Zhu, D.; Bao, X.; Zhu, Q.; Gu, C.; Qiu, M.; Wen, S.; Wang, J.; Shahid, B.; Yang, R. Thienothiophene-Based Copolymers for High-Performance Solar Cells, Employing Different Orientations of the Thiazole Group as a π Bridge. *Energy Environ. Sci.* 2017, *10*, 614−620.
(21) Shi, S.; Yuan, J.; Ding, G.; Ford, M.; Lu, K.; Shi, G.; Sun, J.; Ling, X.; Li, Y.; Ma, W. Improved All-Polymer Solar Cell Performance by Using Matched Polymer Acceptor. *Adv. Funct. Mater.* 2016, *26*, 5669−5678.
(22) Zhao, J.; Li, Y.; Hunt, A.; Zhang, J.; Yao, H.; Li, Z.; Zhang, J.; Huang, F.; Ade, H.; Yan, H. A Difluorobenzoxadiazole Building Block for Efficient Polymer Solar Cells. *Adv. Mater.* 2016, *28*, 1868−1873.
(23) Suman; Gupta, V.; Bagui, A.; Singh, S. P. Molecular Engineering of Highly Efficient Small Molecule Nonfullerene Acceptor for Organic Solar Cells. *Adv. Funct. Mater.* 2017, *27*, 1603820.
(24) Wang, X.; Deng, W.; Chen, Y.; Wang, X.; Ye, P.; Wu, X.; Yan, C.; Zhan, X.; Liu, F.; Huang, H. Fine-Tuning Solid State Packing and Significantly Improving Photovoltaic Performance of Conjugated Polymers through Side Chain Engineering via Random Polymerization. *J. Mater. Chem. A* 2017, *5*, 5585−5593.
(25) Hendriks, K. H.; Heintges, G. H.; Gevaerts, V. S.; Wienk, M. M.; Janssen, R. A. High-Molecular-Weight Regular Alternating Diketopyrrolopyrrole-Based Terpolymers for Efficient Organic Solar Cells. *Angew. Chem., Int. Ed.* 2013, *52*, 8341−8344.
(26) Huang, Y.; Zhang, M.; Chen, H.; Wu, F.; Cao, Z.; Zhang, L.; Tan, S. Efficient Polymer Solar Cells based on Terpolymers with a Broad Absorption Range of 300−900 nm. *J. Mater. Chem. A* 2014, *2*, 5218−5223.
(27) Tamilavan, V.; Roh, K. H.; Agneeswari, R.; Lee, D. Y.; Cho, S.; Jin, Y.; Park, S. H.; Hyun, M. H. Highly Efficient Imide Functionalized Pyrrolo[3,4-*c*]pyrrole-1,3-dione-Based Random Copolymer Containing Thieno[3,4-*c*]pyrrole-4,6-dione and Benzodithiophene for Simple Structured Polymer Solar Cells. *J. Mater. Chem. A* 2014, *2*, 20126−20132.
(28) Lee, J. W.; Ahn, H.; Jo, W. H. Conjugated Random Copolymers Consisting of Pyridine- and Thiophene-Capped Diketopyrrolopyrrole as Co-Electron Accepting Units To Enhance both $J_{SC}$ and $V_{OC}$ of Polymer Solar Cells. *Macromolecules* 2015, *48*, 7836−7842.
(29) Howard, J. B.; Ekiz, S.; Cuellar De Lucio, A. J.; Thompson, B. C. Investigation of Random Copolymer Analogues of a Semi-Random Conjugated Polymer Incorporating Thieno[3,4-*b*]pyrazine. *Macromolecules* 2016, *49*, 6360−6367.
(30) SambathKumar, B.; Shyam Vinod Kumar, P.; Deepakrao, F. S.; Kumar Iyer, S. S.; Subramanian, V.; Datt, R.; Gupta, V.; Chand, S.; Somanathan, N. Two Donor−One Acceptor Random Terpolymer Comprised of Diketopyrrolopyrrole Quaterthiophene with Various Donor π-Linkers for Organic Photovoltaic Application. *J. Phys. Chem. C* 2016, *120*, 26609−26619.
(31) Beaupre,́S.; Shaker-Sepasgozar, S.; Najari, A.; Leclerc, M. Random D−$A_1$−D−$A_2$ Terpolymers based on Benzodithiophene, Thiadiazole[3,4-*e*]isoindole-5,7-dione and Thieno[3,4-*c*]pyrrole-4,6-


DOI: 10.1021/acsami.7b09565
ACS Appl. Mater. Interfaces 2017, 9, 32126−32134

dione for Efficient Polymer Solar Cells. *J. Mater. Chem. A* 2017, *5*, 6638−6647.
(32) Genene, Z.; Wang, J.; Xu, X.; Yang, R.; Mammo, W.; Wang, E. A Comparative Study of the Photovoltaic Performances of Terpolymers and Ternary Systems. *RSC Adv.* 2017, *7*, 17959−17967.
(33) Yang, B.; Zhang, S.; Chen, Y.; Cui, Y.; Liu, D.; Yao, H.; Zhang, J.; Wei, Z.; Hou, J. Investigation of Conjugated Polymers Based on Naphtho[2,3-*c*]thiophene-4,9-dione in Fullerene-Based and Fullerene-Free Polymer Solar Cells. *Macromolecules* 2017, *50*, 1453−1462.
(34) Lim, Y.; Ihn, S.-G.; Bulliard, X.; Yun, S.; Chung, Y.; Kim, Y.; Chang, H.; Choi, Y. S. Controlling Band Gap and Hole Mobility of Photovoltaic Donor Polymers with Terpolymer System. *Polymer* 2012, *53*, 5275−5284.
(35) Nielsen, C. B.; Ashraf, R. S.; Schroeder, B. C.; D'Angelo, P.; Watkins, S. E.; Song, K.; Anthopoulos, T. D.; McCulloch, I. Random Benzotrithiophene-Based Donor-Acceptor Copolymers for Efficient Organic Photovoltaic Devices. *Chem. Commun.* 2012, *48*, 5832−5834.
(36) Kang, T. E.; Cho, H.-H.; Kim, H. j.; Lee, W.; Kang, H.; Kim, B. J. Importance of Optimal Composition in Random Terpolymer-Based Polymer Solar Cells. *Macromolecules* 2013, *46*, 6806−6813.
(37) Hendriks, K. H.; Heintges, G. H. L.; Wienk, M. M.; Janssen, R. A. J. Comparing Random and Regular Diketopyrrolopyrrole-Bithiophene-Thienopyrrolodione Terpolymers for Organic Photovoltaics. *J. Mater. Chem. A* 2014, *2*, 17899−17905.
(38) Lee, J.; Kim, M.; Kang, B.; Jo, S. B.; Kim, H. G.; Shin, J.; Cho, K. Side-Chain Engineering for Fine-Tuning of Energy Levels and Nanoscale Morphology in Polymer Solar Cells. *Adv. Energy Mater.* 2014, *4*, 1400087.
*(39)* Duan, C.; Gao, K.; van Franeker, J. J.; Liu, F.; Wienk, M. M.; Janssen, R. A. Toward Practical Useful Polymers for Highly Efficient Solar Cells via a Random Copolymer Approach. *J. Am. Chem. Soc.* 2016, *138*, 10782−10785.
(40) Fan, Q.; Xu, X.; Liu, Y.; Su, W.; He, X.; Zhang, Y.; Tan, H.; Wang, Y.; Peng, Q.; Zhu, W. Enhancing the Photovoltaic Properties of Low Bandgap Terpolymers based on Benzodithiophene and Phenanthrophenazine by Introducing Different Second Acceptor Units. *Polym. Chem.* 2016, *7*, 1747−1755.
(41) Goker, S.; Hizalan, G.; Aktas, E.; Kutkan, S.; Cirpan, A.; Toppare, L. 2,1,3-Benzooxadiazole, Thiophene and Benzodithiophene based Random Copolymers for Organic Photovoltaics: Thiophene versus Thieno[3,2-*b*]thiophene as π-Conjugated Linkers. *New J. Chem.* 2016, *40*, 10455−10464.
(42) Kang, T. E.; Choi, J.; Cho, H.-H.; Yoon, S. C.; Kim, B. J. Donor-Acceptor Random versus Alternating Copolymers for Efficient Polymer Solar Cells: Importance of Optimal Composition in Random Copolymers. *Macromolecules* 2016, *49*, 2096−2105.
(43) Huo, L.; Ye, L.; Wu, Y.; Li, Z.; Guo, X.; Zhang, M.; Zhang, S.; Hou, J. Conjugated and Nonconjugated Substitution Effect on Photovoltaic Properties of Benzodifuran-Based Photovoltaic Polymers. *Macromolecules* 2012, *45*, 6923−6929.
(44) Kim, J.-H.; Kim, H. U.; Kang, I.-N.; Lee, S. K.; Moon, S.-J.; Shin, W. S.; Hwang, D.-H. Incorporation of Pyrene Units to Improve Hole Mobility in Conjugated Polymers for Organic Solar Cells. *Macromolecules* 2012, *45*, 8628−8638.
(45) Li, H.; Liu, F.; Wang, X.; Gu, C.; Wang, P.; Fu, H. Diketopyrrolopyrrole−Thiophene-Benzothiadiazole Random Copolymers: an Effective Strategy To Adjust Thin-Film Crystallinity for Transistor and Photovoltaic Properties. *Macromolecules* 2013, *46*, 9211−9219.
(46) Kim, K.-H.; Park, S.; Yu, H.; Kang, H.; Song, I.; Oh, J. H.; Kim, B. J. Determining Optimal Crystallinity of Diketopyrrolopyrrole-Based Terpolymers for Highly Efficient Polymer Solar Cells and Transistors. *Chem. Mater.* 2014, *26*, 6963−6970.
(47) Ko, E. Y.; Park, G. E.; Lee, D. H.; Um, H. A.; Shin, J.; Cho, M. J.; Choi, D. H. Enhanced Performance of Polymer Solar Cells Comprising Diketopyrrolopyrrole-Based Regular Terpolymer Bearing Two Different pi-Extended Donor Units. *ACS Appl. Mater. Interfaces* 2015, *7*, 28303−28310.
(48) Deng, P.; Wu, B.; Lei, Y.; Cao, H.; Ong, B. S. Regioregular and Random Difluorobenzothiadiazole Electron Donor-Acceptor Polymer Semiconductors for Thin-Film Transistors and Polymer Solar Cells. *Macromolecules* 2016, *49*, 2541−2548.
(49) Nair, V. S.; Sun, J.; Qi, P.; Yang, S.; Liu, Z.; Zhang, D.; Ajayaghosh, A. Conjugated Random Donor-Acceptor Copolymers of [1]Benzothieno[3,2-*b*]benzothiophene and Diketopyrrolopyrrole Units for High Performance Polymeric Semiconductor Applications. *Macromolecules* 2016, *49*, 6334−6342.
(50) Liao, X.; Zhang, L.; Chen, L.; Hu, X.; Ai, Q.; Ma, W.; Chen, Y. Room Temperature Processed Polymers for High-Efficient Polymer Solar Cells with Power Conversion Efficiency Over 9%. *Nano Energy* 2017, *37*, 32−39.
(51) Huo, L.; Zhang, S.; Guo, X.; Xu, F.; Li, Y.; Hou, J. Replacing Alkoxy Groups with Alkylthienyl Groups: a Feasible Approach to Improve the Properties of Photovoltaic Polymers. *Angew. Chem., Int. Ed.* 2011, *50*, 9697−9702.
(52) Clark, J.; Silva, C.; Friend, R. H.; Spano, F. C. Role of Intermolecular Coupling in the Photophysics of Disordered Organic Semiconductors: Aggregate Emission in Regioregular Polythiophene. *Phys. Rev. Lett.* 2007, *98*, 206406.
(53) Spano, F. C. The Spectral Signatures of Frenkel Polarons in H- and J-Aggregates. *Acc. Chem. Res.* 2010, *43*, 429−439.
(54) Han, L.; Hu, T.; Bao, X.; Qiu, M.; Shen, W.; Sun, M.; Chen, W.; Yang, R. Steric Minimization Towards High Planarity and Molecular Weight for Aggregation and Photovoltaic Studies. *J. Mater. Chem. A* 2015, *3*, 23587−23596.
(55) Zhai, L.; Liu, M.; Xue, P.; Sun, J.; Gong, P.; Zhang, Z.; Sun, J.; Lu, R. Nanofibers Generated from Nonclassical Organogelators based on Difluoroboron β-Diketonate Complexes to Detect Aliphatic Primary Amine Vapors. *J. Mater. Chem. C* 2016, *4*, 7939−7947.
(56) Eckstein, B. J.; Melkonyan, F. S.; Zhou, N.; Manley, E. F.; Smith, J.; Timalsina, A.; Chang, R. P. H.; Chen, L. X.; Facchetti, A.; Marks, T. J. Buta-1,3-diyne-Based π-Conjugated Polymers for Organic Transistors and Solar Cells. *Macromolecules* 2017, *50*, 1430−1441.
(57) Carsten, B.; Szarko, J. M.; Son, H. J.; Wang, W.; Lu, L.; He, F.; Rolczynski, B. S.; Lou, S. J.; Chen, L. X.; Yu, L. Examining the Effect of the Dipole Moment on Charge Separation in Donor-Acceptor Polymers for Organic Photovoltaic Applications. *J. Am. Chem. Soc.* 2011, *133*, 20468−20475.
(58) Carsten, B.; Szarko, J. M.; Lu, L.; Son, H. J.; He, F.; Botros, Y. Y.; Chen, L. X.; Yu, L. Mediating Solar Cell Performance by Controlling the Internal Dipole Change in Organic Photovoltaic Polymers. *Macromolecules* 2012, *45*, 6390−6395.
(59) Guo, X.; Zhou, N.; Lou, S. J.; Smith, J.; Tice, D. B.; Hennek, J. W.; Ortiz, R. P.; Navarrete, J. T. L.; Li, S.; Strzalka, J.; Chen, L. X.; Chang, R. P. H.; Facchetti, A.; Marks, T. J. Polymer Solar Cells with Enhanced Fill Factors. *Nat. Photonics* 2013, *7*, 825−833.
(60) Li, J.; Wang, X.; Du, S.; Tong, J.; Zhang, P.; Guo, P.; Yang, C.; Xia, Y. A Two-dimension Medium Band Gap Conjugated Polymer Based on 5,10-bis(alkylthien-2-yl)dithieno[3,2-*d*:3′,2′-*d*′]benzo[1,2-*b*:4,5-*b*′]dithiophene: Synthesis and Photovoltaic Application. *J. Macromol. Sci., Part A: Pure Appl.Chem.* 2016, *53*, 538−545.
(61) Cowan, S. R.; Roy, A.; Heeger, A. J. Recombination in Polymer-Fullerene Bulk Heterojunction Solar Cells. *Phys. Rev. B: Condens. Matter Mater. Phys.* 2010, *82*, 245207.
(62) Wang, K.; Yi, C.; Liu, C.; Hu, X.; Chuang, S.; Gong, X. Effects of Magnetic Nanoparticles and External Magnetostatic Field on the Bulk Heterojunction Polymer Solar Cells. *Sci. Rep.* 2015, *5*, 9265.
(63) Schaffer, C. J.; Palumbiny, C. M.; Niedermeier, M. A.; Burger, C.; Santoro, G.; Roth, S. V.; Müller-Buschbaum, P. Morphological Degradation in Low Bandgap Polymer Solar Cells-An In Operando Study. *Adv. Energy Mater.* 2016, *6*, 1600712.
(64) Li, Y.; Yang, Y.; Bao, X.; Qiu, M.; Liu, Z.; Wang, N.; Zhang, G.; Yang, R.; Zhang, D. New π-conjugated Polymers as Acceptors Designed for all Polymer Solar Cells Based on Imide/Amide-derivatives. *J. Mater. Chem. C* 2016, *4*, 185−192.
(65) Zhu, D.; Sun, L.; Bao, X.; Wen, S.; Han, L.; Gu, C.; Guo, J.; Yang, R. Low Band-gap Polymers Based on Easily Synthesized


DOI: 10.1021/acsami.7b09565
*ACS Appl. Mater. Interfaces* 2017, 9, 32126−32134

Thioester-substituted Thieno[3,4-*b*]thiophene for Polymer Solar Cells.
*RSC Adv.* 2015, *5*, 62336−62342.



DOI: 10.1021/acsami.7b09565
*ACS Appl. Mater. Interfaces* 2017, 9, 32126−32134